Polyhedron 178 (2020) 114332

Contents lists available at ScienceDirect

Polyhedron

journal homepage: www.elsevier.com/locate/poly

Blue-phosphorescent bis-cyclometalated iridium complexes with aryl isocyanide ancillary ligands

Louise M. Cañada, Johanna Kölling, Thomas S. Teets *

University of Houston, Department of Chemistry, 3585 Cullen Blvd., Room 112, Houston, TX 77204-5003, USA

ARTICLE INFO

Article history:
Received 2 December 2019
Accepted 22 December 2019
Available online 25 December 2019

Keywords:
Cyclometalated iridium
Isocyanide
Blue photoluminescence
Photophysics
Phosphorescence

ABSTRACT

The design of organometallic complexes with efficient blue phosphorescence remains a challenge in the field of optoelectronics. This paper describes a series of eight cationic, isocyanide-ligated bis-cyclometalated iridium complexes of the general formula $[Ir(C^Y)_2(CNAr)_2](PF_6)$, where C^Y is a triazole-based C^N cyclometalating ligand or an NHC-based C^C: cyclometalating ligand, and CNAr is an aryl isocyanide. The triazole- and NHC-derived cyclometalating ligands, in combination with the π-acidic isocyanide ancillary ligands, result in large HOMO–LUMO gaps and engender these compounds with photoluminescence in the blue region of the spectrum. The complexes are synthesized by a general synthetic procedure and isolated in moderate to good isolated yields, with a combination of NMR spectroscopy, mass spectrometry, and X-ray crystallography (for six of the eight compounds) establishing the identity and bulk purity of each compound. The redox properties of the compounds are studied by cyclic voltammetry, which provide evidence for the large HOMO–LUMO gaps that are critical for the blue photoluminescence. The triazole-based compounds are weakly luminescent in fluid solution at room temperature, and all complexes luminesce at 77 K in frozen solvent glass or at room temperature when immobilized in a transparent poly (methyl methacrylate) (PMMA) film. CIE coordinates for the photoluminescence spectra indicate pure blue emission for all compounds, with CIEy $\leq$ 0.15 for all but one compound.

1. Introduction

Cyclometalated iridium complexes are among the most successful classes of organometallic compounds in many photochemical applications [1], and they have been especially prominent in the design of organic light-emitting diodes (OLEDs) [2]. Like most luminescent heavy transition-metal organometallic compounds, cyclometalated iridium complexes luminesce from triplet excited states, and they are thus able to efficiently harvest both singlet and triplet excitons in electroluminescent devices, improving device efficiency. In addition, among phosphorescent emitters cyclometalated iridium complexes are particularly robust, their phosphorescence color can be easily tuned, and the large spin–orbit coupling of iridium results in very fast triplet radiative decay and thus very high photoluminescence quantum yields, making them ideal choices for display applications. Acknowledging that some of the first research on cyclometalated iridium involved heteroleptic bis-cyclometalated structures [3,4], much of the early work on cyclometalated iridium compounds focused on homoleptic compounds of the type $Ir(C^N)_3$ [5], usually in a *fac* geometry, where C^N is the cyclometalating ligand. In addition to being among the first class of cyclometalated iridium complexes to be widely studied, these homoleptic compounds have found academic and commercial success in OLED devices [6,7]. It was recognized soon after that heteroleptic bis-cyclometalated iridium complexes of the general formula $Ir(C^N)_2(L^X)$, where L^X is a monoanionic ancillary ligand, present some advantages in the design of OLED emitters, and these have been used extensively since the early 2000's [8–11]. In addition to often being easier to synthesize than the homoleptic $Ir(C^N)_3$ analogues, the ancillary ligand(s) in heteroleptic bis-cyclometalated iridium complexes offer an additional layer of control over the photoluminescence and excited-state dynamics, a feature that has been exploited extensively by our group [12–15] and several others [16,17].

In cyclometalated iridium phosphors, the color of the photoluminescence is controlled primarily by the choice of cyclometalating ligand, and it is possible to span the entire visible range and even beyond. Most OLED display applications use three primary colors, requiring red, green, and blue (RGB) to operate. Cyclometalated iridium complexes have found commercial success in red and green devices, but there are no blue-phosphorescent iridium complexes (or complexes of any other metal) that are efficient and stable enough to be applied in a commercial device. As such, there

* Corresponding author.
E-mail address: tteets@uh.edu (T.S. Teets).

https://doi.org/10.1016/j.poly.2019.114332
0277-5387/

is continued effort to design and study new types of cyclometalated iridium complexes with the requisite color purity, quantum efficiency, and stability to function in OLED devices. Most recent efforts to design improved blue-phosphorescent iridium complexes have involved modifications to the cyclometalating ligand, aimed at improving the color profile and/or photostability of the compound. A particularly successful approach has been to use C^C: cyclometalating ligands derived from *N*-heterocyclic carbenes (NHCs), replacing the ubiquitous C^N cyclometalating ligands. This approach was introduced over 15 years ago, and most complexes in this class have been homoleptic Ir(C^C:)$_3$ varieties [18–23], although there have been a few examples of heteroleptic bis-cyclometalated iridium complexes with C^C: ligands [24–26]. In addition, our group has shown that related acyclic diaminocarbenes (ADCs), installed as ancillary ligands on C^N [27,28] or C^C: [29] bis-cyclometalated iridium complexes, are a promising design element for blue phosphorescence. Another class of C^N cyclometalating ligand, which is comparatively underdeveloped but has been used successfully in blue-emitting complexes, is the 5-aryl-1,2,4-triazolyl family, which is accessed in a one-pot procedure from the corresponding benzoyl chloride derivative, allowing easy modification of the aryl group as a means of controlling the photoluminescence wavelength [30]. These ligands have mostly been used to synthesize homoleptic Ir(C^N)$_3$ complexes which can be processed into dendrimeric structures [31,32], and they result in photoluminescence in the blue region of the spectrum. Considering that most of the recent successes in blue-phosphorescent iridium complexes have been homoleptic structures, there has been less effort involving ancillary ligand design in blue-emitting bis-cyclometalated iridium complexes. That said, we [33,34] and others [16,35–38] have shown that isocyanides, which stabilize the Ir dπ HOMO by virtue of their π-acidity, are a good choice for blue-phosphorescent complexes in that they increase the HOMO–LUMO gap and improve chemical stability.

Given the success of NHC and triazolyl cyclometalating ligands in supporting blue-phosphorescent complexes, we became interested in exploring combinations of these cyclometalating ligands with aryl isocyanide ancillary ligands. In this work, we introduce several blue-phosphorescent bis-cyclometalated iridium complexes supported by aryl isocyanide ancillary ligands. The compounds are all cationic with the general structure [Ir(C^Y)$_2$(CNAr)$_2$]$^+$, where C^Y is either a 5-aryl-1,2,4-triazolyl C^N cyclometalating ligand or an NHC-based C^C: cyclometalating ligand. We include two different aryl isocyanides (CNAr) in this study – the sterically encumbered and more electron-rich 2,6-dimethylphenyl isocyanide (CNAr^{dmp}), and the electron-accepting isocyanide 4-trifluoromethylphenyl isocyanide (CNAr$^{4\text{-}CF3}$). The synthetic chemistry, molecular structures, and redox properties of these compounds are elaborated, and studies of their photoluminescence spectra show that most members of this series exhibit efficient blue phosphorescence with good color purity. The spectral profile, quantum yield, and lifetime all depend primarily on the choice of cyclometalating ligand, with only subtle effects of the isocyanide.

2. Material and methods

2.1. Materials

All reactions were performed in a nitrogen-filled glovebox. Solvents for reactions and optical measurements were obtained from a Grubbs solvent purification system and degassed with argon. Commercially available starting materials and reagents were used without further purification. Chloro-bridged Ir dimers of the general formula [Ir(C^Y)$_2$(μ-Cl)]$_2$ (C^Y = cyclometalating ligand) and 4-trifluoromethylphenyl isocyanide (CNAr$^{4\text{-}CF3}$) were synthesized following previously reported procedures and used without further purification [30,39,40]. Due to its instability, the CNAr$^{4\text{-}CF3}$ ligand was carried forward to the next synthetic step immediately following preparation, and measured amounts for this ligand are approximate.

2.2. Physical methods

^{1}H, ^{19}F, and ^{13}C{^{1}H} NMR spectra were recorded at room temperature using a JEOL ECA-500 or ECA-600 NMR spectrometer. The static nanoESI-MS experiments were carried out using a Thermo Exactive mass spectrometer and operated in positive ionization mode, with a spray voltage of 1.5 kV. UV–vis absorption spectra were recorded in dichloromethane solutions in screw-capped 1 cm quartz cuvettes using an Agilent Carey 8454 UV–vis spectrophotometer. Steady-state emission and excitation spectra were recorded using a Horiba FluoroMax-4 spectrofluorometer. To exclude air, samples for emission spectra were prepared in a nitrogen-filled glovebox using dry, deoxygenated solvents, and thin-film PMMA samples were kept under nitrogen until immediately before measurement. Samples for room-temperature emission were housed in 1 cm quartz cuvettes with septum-sealed screw caps, and samples for low-temperature emission were contained in a custom quartz EPR tube with high-vacuum valve and immersed in liquid nitrogen using a finger Dewar. Emission quantum yields were determined relative to a standard of quinine sulfate in 0.05 M sulfuric acid, which has a reported fluorescence quantum yield (Φ_F) of 0.52 [41]. The absolute quantum yields of complexes doped into poly(methyl methacrylate) (PMMA) thin films were recorded using a Spectralon-coated integrating sphere integrated with a Horiba FluoroMax-4 spectrofluorometer. Phosphorescence lifetimes were measured on a Horiba DeltaFlex Lifetime System using 330 nm excitation. Cyclic voltammetry (CV) experiments were performed with a CH Instruments 602E potentiostat using a three-electrode system in a nitrogen-filled glovebox. A 3 mm diameter glassy-carbon electrode, Pt wire, and silver wire were used as working electrode, counter electrode, and pseudoreference electrode, respectively. Measurements were carried out in acetonitrile solution with 0.1 M TBAPF$_6$ as a supporting electrolyte at a scan rate of 0.1 V/s. Ferrocene was used as an internal standard, and potentials were referenced to the ferrocene/ferrocenium couple. NMR spectra of all new compounds (see Figs. S6–S21 in the Supplementary Material) provide evidence for bulk purity.

2.3. PMMA film fabrication

A solution of PMMA (98–147 mg, 35 kDa) in dichloromethane (1.0 mL) was stirred at room temperature in a nitrogen-filled glovebox. Then, the respective iridium complex (2–3 mg, 2 wt%) was added to the solution and stirred, giving a homogeneous solution. The resulting solution was drop-coated on a quartz substrate and dried at room temperature overnight.

2.4. X-ray crystallography details

Single crystals were grown by layering CH_2Cl_2 or $CHCl_3$ solutions with hexane or diethyl ether. Crystals were mounted on a Bruker Apex II three-circle diffractometer using MoKα radiation (λ = 0.71073 Å). The data were collected at 123(2) K and processed and refined within the APEXII software. Structures were solved using intrinsic phasing methods in SHELXT and refined by standard difference Fourier techniques in the program SHELXL [42]. Hydrogen atoms were placed in calculated positions using the standard riding model and refined isotropically. All non-hydrogen atoms were refined anisotropically. In the structure of **1** there were three

crystallographically independent molecules and several disordered parts, namely two propyl groups on F_2ptz ligands, two CF_3 groups on $CNAr^{4\text{-}CF3}$ ligands, one entire 4-trifluoromethylphenyl group, and two of the three PF_6^- counterions. The structures of **2** and **4** also include one disordered propyl group each, in **3** the PF_6^- and CH_2Cl_2 solvate are disordered, and in **7** a CF_3 group and CH_2Cl_2 solvent molecule are disordered. Distance restraints were used to affix the 1,2 and 1,3, distances in the disordered parts, and rigid bond restraints (SIMU and DELU) were used for the thermal ellipsoid parameters. In addition, the structures of **1**, **2**, and **4** included heavily disordered electron density assigned to additional solvent molecules in the structure that could not be satisfactorily modeled, necessitating the use of the SQUEEZE function in PLATON [43]. Crystallographic details are summarized in Tables S1 and S2.

2.5. General procedure for the preparation of complexes

The chloro-bridged Ir dimer was dissolved or suspended in CH_2Cl_2 and combined with 2 equiv of $AgPF_6$. The resulting reaction mixture was mixed with 4 eq of 2,6-dimethylphenyl isocyanide ($CNAr^{dmp}$) or 4-trifluoromethylphenyl isocyanide ($CNAr^{4\text{-}CF3}$) and stirred at room temperature, overnight. The completed reaction mixture was filtered through Celite to remove AgCl. The filtrate volume was reduced and hexane or diethyl ether was added to induce precipitation. The solid was dried under vacuum. The resulting crude product was purified either by precipitation or by recrystallization from CH_2Cl_2/hexane or $CHCl_3$/diethyl ether to give a white solid or colorless crystals.

$[Ir(F_2ptz)_2(CNAr^{4\text{-}CF3})_2]PF_6$ (1). Prepared by the general procedure, using $[Ir(F_2ptz)_2(\mu\text{-}Cl)]_2$ (406 mg, 0.290 mmol), $AgPF_6$ (147 mg, 0.580 mmol), and 4-trifluoromethylphenyl isocyanide (~200 mg, ~4 equiv, 1.2 mmol). The resulting product was purified by precipitation from CH_2Cl_2/hexane to give a white solid. Yield: 228 mg, 34%. ^{1}H NMR (600 MHz, CD_2Cl_2) δ: 7.75 (d, J = 8.2 Hz, 4H, Ar*H*), 7.54 (d, J = 7.6 Hz, 4H, Ar*H*), 6.65 (t, J = 9.6 Hz, 2H, Ar*H*), 5.88 (d, J = 6.9 Hz, 2H, Ar*H*), 4.39 (d, J = 6.9 Hz, 6H, NCH_3), 2.97–2.88 (m, 4H, CCH_2CH$_2$CH$_3$), 1.91 (d, J = 6.2 Hz, 4H, CCH$_2$CH_2-CH$_3$), 0.96 (t, J = 6.5 Hz, 6H, CCH$_2$CH$_2$CH_3). ^{19}F NMR (565 MHz, CD_2Cl_2) δ: −62.99 (s, 6F, CF_3), −72.29 (d, J = 711.2 Hz, 6F, PF_6), −100.72 (d, J = 8.9 Hz, 2F, Ar*F*), −103.33 (q, J = 8.4 Hz, 2F, Ar*F*). HRMS-ESI (m/z): $[M-PF_6]^+$ calcd for $C_{40}H_{32}F_{16}IrN_8P$, 1007.22195; found, 1007.22217.

$[Ir(F_2ptz)_2(CNAr^{dmp})_2]PF_6$ (2). Prepared by the general protocol, using $[Ir(F_2ptz)_2(\mu\text{-}Cl)]_2$ (200 mg, 0.143 mmol), $AgPF_6$ (71 mg, 0.28 mmol) and 2,6-dimethylphenyl isocyanide (74 mg, 0.56 mmol). The product was purified by precipitation and recrystallization to form a colorless solid, which was dried in vacuo. Yield: 241 mg, 80%. ^{1}H NMR (600 MHz, $CDCl_3$) δ: 7.25 (t, J = 7.6 Hz, 2H, Ar*H*), 7.14 (d, J = 7.6 Hz, 4H, Ar*H*), 6.62 (m, 2H, Ar*H*), 5.84 (dd, J = 7.6, 2.8 Hz, 2H, Ar*H*), 4.39 (d, J = 7.6 Hz, 6H, NCH_3), 2.86–2.77 (m, 4H, CCH_2CH$_2$CH$_3$), 2.12 (s, 12H, ArCH_3), 1.91–1.77 (m, 4H, CCH$_2$CH_2CH$_3$), 0.83 (t, J = 7.6 Hz, 6H, CCH$_2$CH$_2$-CH_3). ^{19}F NMR (565 MHz, $CDCl_3$) δ: −73.85 (d, J = 712.0 Hz, 6F, PF_6), −100.52 to − 100.44 (m, 2F, Ar*F*), −102.34 (dd, J = 18.6, 8.1 Mz, 2F, Ar*F*). HRMS-ESI (m/z): $[M-PF_6]^+$ calcd for $C_{42}H_{42}F_{10}IrN_8P$, 927.30923; found, 927.30920.

$[Ir(CF_3ptz)_2(CNAr^{4\text{-}CF3})_2]PF_6$ (3). Following the described general procedure, $[Ir(CF_3ptz)_2(\mu\text{-}Cl)]_2$ (384 mg, 0.251 mmol), $AgPF_6$ (127 mg, 0.502 mmol), and 4-trifluoromethylphenyl isocyanide (~172 mg, 1 mmol, 4 equiv) were allowed to react to afford a white solid. The product was purified by recrystallization from CH_2Cl_2/hexane. Yield: 241 mg, 39%. ^{1}H NMR (600 MHz, CD_2Cl_2) δ: 7.84 (s, 2H, Ar*H*), 7.73 (d, J = 8.9 Hz, 4H, Ar*H*), 7.50 (d, J = 8.2 Hz, 4H, Ar*H*), 7.31 (d, J = 8.2 Hz, 2H, Ar*H*), 6.55 (d, J = 8.2 Hz, 2H, Ar*H*), 4.39 (s, 6H, NCH_3), 2.96 (td, J = 15.5, 7.6 Hz, 4H, CCH_2CH$_2$CH$_3$), 1.96–1.91 (m, 4H, CCH$_2$CH_2CH$_3$), 0.97 (t, J = 7.6 Hz, 6H, CCH$_2$CH$_2$-CH_3). ^{19}F NMR (565 MHz, CD_2Cl_2) δ: −62.68 (s, 6F, CF_3), −63.35 (s, 6F, CF_3), −72.65 (d, J = 711.2 Hz, 6F, PF_6). HRMS-ESI (m/z): $[M-PF_6]^+$ calcd for $C_{42}H_{34}F_{18}IrN_8P$, 1071.23441; found, 1071.23486.

$[Ir(CF_3ptz)_2(CNAr^{dmp})_2]PF_6$ (4). Prepared by the general protocol, using $[Ir(CF_3ptz)_2(\mu\text{-}Cl)]_2$ (100 mg, 0.0654 mmol), $AgPF_6$ (33 mg, 0.13 mmol) and 2,6-dimethylphenyl isocyanide (34 mg, 0.26 mmol). The product was purified by precipitation and recrystallization to form colorless crystals, which were dried in vacuo. Yield: 105 mg, 71%. ^{1}H NMR (600 MHz, $CDCl_3$) δ: 7.81 (s, 2H, Ar*H*), 7.31 (d, J = 8.2 Hz, 2H, Ar*H*), 7.21 (t, J = 7.6 Hz, 2H, Ar*H*), 7.10 (d, J = 7.6 Hz, 4H, Ar*H*), 6.58 (d, J = 8.2 Hz, 2H, Ar*H*), 4.40 (s, 6H, NCH_3), 2.89–2.80 (m, 4H, CCH_2CH$_2$CH$_3$), 2.06 (s, 12H, ArCH_3), 1.92–1.80 (m, 4H, CCH$_2$CH_2CH$_3$), 0.83 (t, J = 7.2 Hz, 6H, CCH$_2$CH$_2$-CH_3). ^{19}F NMR (565 MHz, $CDCl_3$) δ: −62.35 (s, 6F, CF_3), −73.81 (d, J = 712.8 Hz, 6F, PF_6). HRMS-ESI (m/z): $[M-PF_6]^+$ calcd for $C_{44}H_{44}F_{12}IrN_8P$, 991.32169; found, 991.32227.

$[Ir((CF_3)_2ptz)_2(CNAr^{dmp})_2]PF_6$ (5). Prepared by the general protocol, using $[Ir((CF_3)_2ptz)_2(\mu\text{-}Cl)]_2$ (75 mg, 0.042 mmol), $AgPF_6$ (21 mg, 0.084 mmol) and 2,6-dimethylphenyl isocyanide (22 mg, 0.17 mmol). The product was purified by precipitation and recrystallization to form a colorless solid, which was dried in vacuo. Yield: 86 mg, 81%. ^{1}H NMR (600 MHz, $CDCl_3$) δ: 7.97 (s, 2H, Ar*H*), 7.73 (s, 2H, Ar*H*), 7.26 (t, J = 7.6 Hz, 2H, Ar*H*), 7.14 (d, J = 8.3 Hz, 4H, Ar*H*), 4.34 (s, 6H, NCH_3), 2.86 (m, 4H, CCH_2CH$_2$CH$_3$), 2.11 (s, 12H, ArCH_3), 1.92 (m, 4H, CCH$_2$CH_2CH$_3$), 0.87 (t, J = 7.6 Hz, 6H, CCH$_2$CH$_2$CH_3). ^{19}F NMR (565 MHz, $CDCl_3$) δ: −59.73 (s, 6F, CF_3), −62.78 (s, 6F, CF_3), −73.85 (d, J = 712.0 Hz, 6F, PF_6). HRMS-ESI (m/z): $[M-PF_6]^+$ calcd for $C_{46}H_{42}F_{18}IrN_8P$, 1127.29646; found, 1127.29639.

$[Ir(CF_3pmi)_2(CNAr^{4\text{-}CF3})_2]PF_6$ (6). The reaction was performed with $[Ir(CF_3pmi)_2(\mu\text{-}Cl)]_2$ (308 mg, 0.227 mmol), $AgPF_6$ (115 mg, 0.454 mmol), and 4-trifluoromethylphenyl isocyanide (~155 mg, 0.908 mmol, 4 equiv) according to the general procedure. The crude product was purified by recrystallization from $CHCl_3$/diethyl ether to afford colorless crystals. Yield: 138 mg, 27%. ^{1}H NMR (600 MHz, CD_2Cl_2) δ: 7.74 (d, J = 2.1 Hz, 2H, Ar*H*), 7.69 (d, J = 8.2 Hz, 4H, Ar*H*), 7.45 (s, 4H, Ar*H*), 7.44 (s, 2H, Ar*H*), 7.41 (d, J = 2.1 Hz, 2H, Ar*H*), 7.01 (d, J = 7.6 Hz, 2H, Ar*H*), 6.54 (d, J = 7.6 Hz, 2H, Ar*H*), 4.18 (s, 6H, NCH_3). ^{19}F NMR (565 MHz, CD_2Cl_2) δ: −60.06 (s, 6F, CF_3), −61.00 (s, 6F, CF_3), −70.18 (d, J = 710.8 Hz, 6F, PF_6). HRMS-ESI (m/z): $[M-PF_6]^+$ calcd for $C_{38}H_{24}F_{18}IrN_6P$, 985.15001; found, 985.15002.

$[Ir(CF_3pmi)_2(CNAr^{dmp})_2]PF_6$ (7). Following the general protocol, $[Ir(CF_3pmi)_2(\mu\text{-}Cl)]_2$ (400 mg, 0.295 mmol), $AgPF_6$ (152 mg, 0.601 mmol) and 2,6-dimethylphenylisocyanide (157 mg, 1.20 mmol) were combined. The product was purified by dissolving in DCM and filtering through silica. Afterwards the product was recrystallized to form colorless crystals. Yield: 239 mg, 38%. ^{1}H NMR (500 MHz, CD_2Cl_2) δ: 7.73 (s, 2H, Ar*H*), 7.44 (s, 2H, Ar*H*), 7.40 (s, 2H, Ar*H*), 7.19 (t, J = 7.7 Hz, 2H, Ar*H*), 7.07 (d, J = 8.0 Hz, 4H, Ar*H*), 7.01 (d, J = 7.4 Hz, 2H, Ar*H*), 6.61 (d, J = 7.4 Hz, 2H, Ar*H*), 4.12 (s, 6H, NCH_3), 2.03 (s, 12H, ArCH_3). ^{19}F NMR (470 MHz, CD_2Cl_2) δ: −62.4 (s, 6F, CF_3), −73.2 (d, J = 710.8 Hz, 6F, PF_6). HRMS-ESI (m/z): $[M-PF_6]^+$ calcd for $C_{40}H_{34}F_{12}IrN_6P$, 905.23729; found, 905.23322.

$[Ir(pmi)_2(CNAr^{dmp})_2]PF_6$ (8). Following the general procedure, $[Ir(pmi)_2(\mu\text{-}Cl)]_2$ (200 mg, 0.184 mmol), $AgPF_6$ (93 mg, 0.37 mmol), and 2,6-dimethylphenyl isocyanide (97 mg, 0.74 mmol) were allowed to react to give a white product, which was purified by recrystallization from $CHCl_3$/diethyl ether. Yield: 312 mg, 93%. ^{1}H NMR (600 MHz, CD_2Cl_2) δ: 7.69 (d, J = 1.7 Hz, 2H, Ar*H*), 7.36 (d, J = 2.3 Hz, 2H, Ar*H*), 7.26 (d, J = 8.0 Hz, 2H, Ar*H*), 7.19 (t, J = 7.7 Hz, 2H, Ar*H*), 7.09 (d, J = 7.4 Hz, 4H, Ar*H*), 7.03 (t, J = 7.7 Hz, 2H, Ar*H*), 6.77 (t, J = 7.2 Hz, 2H, Ar*H*), 6.51 (d, J = 6.9 Hz, 2H, Ar*H*), 4.12 (s, 6H, NCH_3), 2.06 (s, 12H, ArCH_3). ^{13}C

{^{1}H} NMR (151 MHz, CD_2Cl_2) δ: 161.2, 146.4, 137.0, 135.4, 133.6, 131.3, 129.8, 128.5, 127.1, 126.8, 124.5, 123.4, 116.3, 112.5, 39.1, 18.3. HRMS-ESI (m/z): $[M-PF_6]^+$ calcd for $C_{38}H_{36}F_6IrN_6P$, 769.26307; found, 769.26306.

3. Results and discussion

3.1. Synthesis

Eight cationic bis-cyclometalated iridium bis-isocyanide complexes were prepared by the general method described in Scheme 1, analogous to procedures previously used by our group to prepare related complexes [33,34]. In this reaction, the chloride-bridged dimer $[Ir(C^Y)_2(\mu\text{-}Cl)]_2$ is treated sequentially with 2 equiv of $AgPF_6$ and 4 equiv of the aryl isocyanide in dichloromethane, and room-temperature reaction furnishes the desired product, which is purified by precipitation or recrystallization. To assemble the eight complexes described here, five different cyclometalating ligands and two different isocyanides were used. Three of the cyclometalating ligands – F_2ptz, CF_3ptz, and $(CF_3)_2$ptz – are members of the 5-aryl-1,2,4-triazolyl family with differential substitution on the aryl ring, and the others – CF_3pmi and pmi – are both NHC-based 1-methyl-3-aryl-imidazol-2-ylidine cyclometalating ligands. These are combined with the aryl isocyanide ligands 2,6-dimethylphenyl isocyanide ($CNAr^{dmp}$), a commercially available and easy-to-handle solid, and 4-trifluoromethylphenyl isocyanide ($CNAr^{4\text{-}CF3}$), which we must prepare and immediately use. We noted in previous work that the electronic nature of the isocyanide has little effect on photoluminescence [33,34], but is critical for reactions that further derivatize the isocyanides into carbene-containing structures [27-29]. Thus, $CNAr^{dmp}$ is the best choice for preparing compounds where the bis(aryl isocyanide) structure is the end goal, but the complexes with $CNAr^{4\text{-}CF3}$ offer the promise of further synthetic elaboration. The instability of $CNAr^{4\text{-}CF3}$ and the difficulty of controlling stoichiometry likely contribute to the lower isolated yields obtained with this isocyanide, but all eight complexes were obtained in satisfactory amounts for further analysis, and their identity and purity confirmed by HRMS and multinuclear NMR. NMR spectroscopy confirms the C_2 symmetry of the products, with a single set of resonances observed for the two cyclometalating ligands and for the two isocyanides.

3.2. X-ray crystal structures

Single-crystal X-ray diffraction confirms the structures of six of the eight complexes, all but **5** and **6** which we were unable to obtain as single crystals. The structures are depicted in Fig. 1 below, in each case showing one crystallographically independent molecule and omitting the PF_6^- counterion and any solvent molecules. In all cases, the neutral "L" donor of the cyclometalating ligand, the triazole in **1**–**4** and the NHC in **7** and **8**, are arranged in a trans disposition, and the isocyanides are *cis* oriented. Surveying the structures, while there is some small variation in the isocyanide C≡N distances and C≡N–C(aryl) bond angles across the series, these values do not seem to vary systematically as a function of the C^Y ligand. In both the triazole and NHC analogues, the isocyanide C≡N internuclear distances are short (≤1.17 Å) and the angles are close to linear (≥169°), indicating relatively little π backbonding into the isocyanide. In addition, the isocyanide bond metrics do not seem to differ between the $CNAr^{4\text{-}CF3}$ and $CNAr^{dmp}$ members of the series. In most cases, the isocyanide aryl ring is rotated into a staggered conformation relative to metal–ligand bonds that lie in the plane perpendicular to the C≡N axis, but there is a variation in conformations among the compounds that suggests the isocyanide can freely rotate, which is consistent with the NMR spectroscopy in solution.

3.3. Electrochemistry

Fig. 2 shows cyclic voltammograms of all compounds reported here. As we have observed for other cationic bis-isocyanide cyclometalated iridium complexes [33,34], redox features for these compounds are typically irreversible. For the aryl-triazolyl complexes **1**–**5**, there are no clearly resolved oxidation waves in the CV within the MeCN solvent window, out to ~ +1.6 V vs the ferrocenium/ferrocene (Fc^+/Fc) couple. This observation indicates that the HOMOs in these compounds are stabilized relative to most other bis-cyclometalated iridium complexes, which typically have well-defined, often reversible Ir^{IV}/Ir^{III} couples occurring at < 1 V vs. Fc^+/Fc. Similar behavior was observed in other cationic bis-isocyanide compounds from our group with fluorinated C^N ligands, which are likewise difficult to oxidize and don't give a clear wave when sweeping anodically in the CV [33,34]. The electronic effect

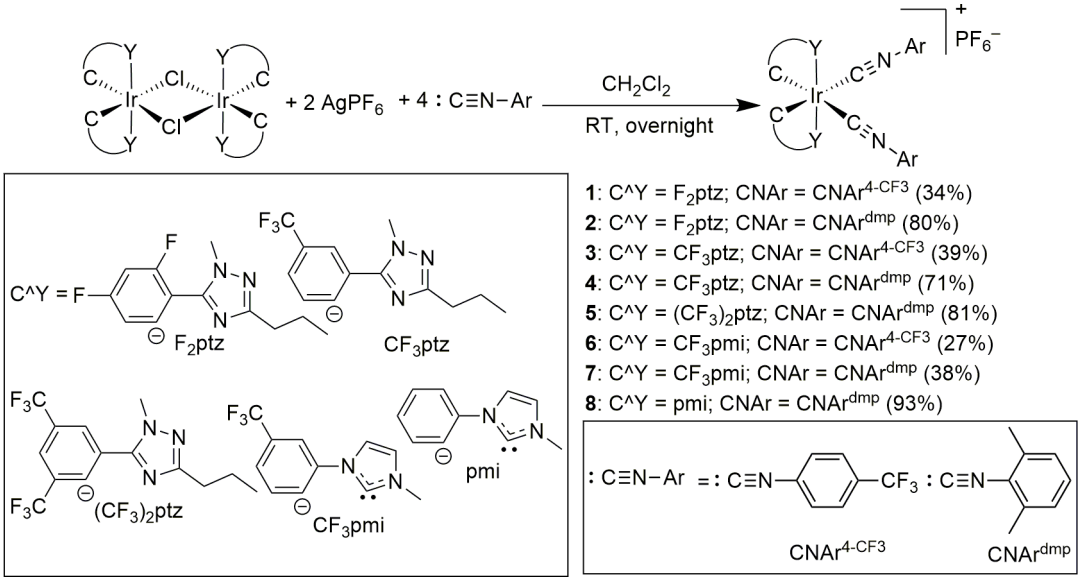

1: C^Y = F_2ptz; CNAr = $CNAr^{4\text{-}CF3}$ (34%)
2: C^Y = F_2ptz; CNAr = $CNAr^{dmp}$ (80%)
3: C^Y = CF_3ptz; CNAr = $CNAr^{4\text{-}CF3}$ (39%)
4: C^Y = CF_3ptz; CNAr = $CNAr^{dmp}$ (71%)
5: C^Y = $(CF_3)_2$ptz; CNAr = $CNAr^{dmp}$ (81%)
6: C^Y = CF_3pmi; CNAr = $CNAr^{4\text{-}CF3}$ (27%)
7: C^Y = CF_3pmi; CNAr = $CNAr^{dmp}$ (38%)
8: C^Y = pmi; CNAr = $CNAr^{dmp}$ (93%)

Scheme 1. Synthesis of bis-isocyanide complexes **1**–**8**.

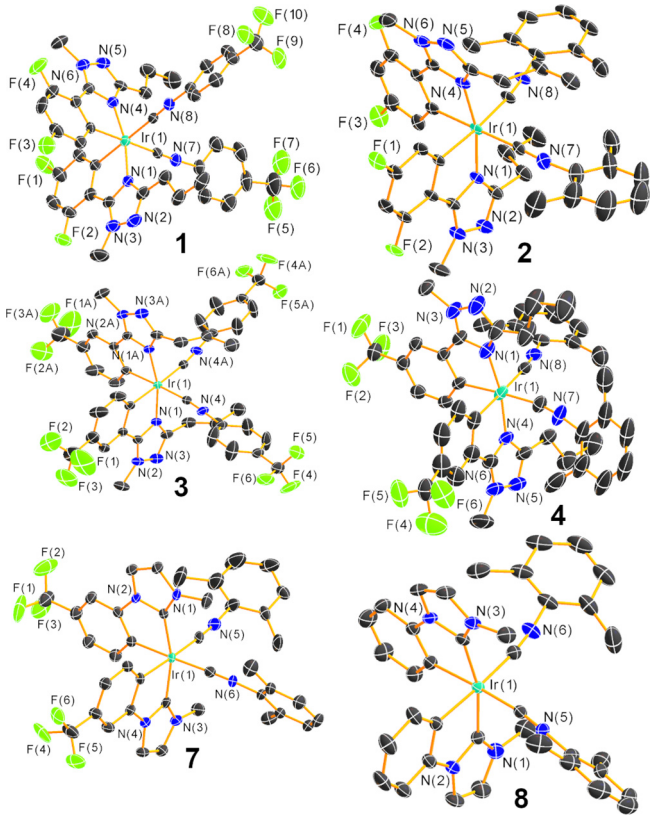

Fig. 1. Molecular structures of **1**–**4**, **7**, and **8**, determined by single-crystal X-ray diffraction. Ellipsoids are shown at the 50% probability level with hydrogen atoms and solvent molecules omitted.

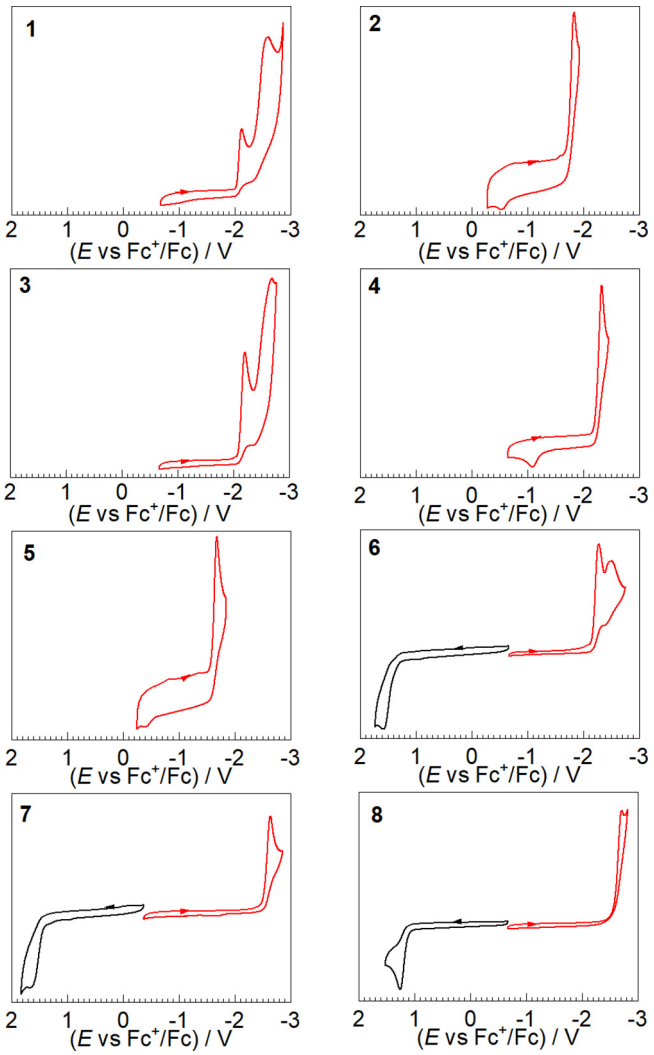

Fig. 2. Cyclic voltammograms of complexes **1**–**8**, recorded in MeCN with 0.1 $TBAPF_6$ as the supporting electrolyte. A glassy carbon working electrode, platinum wire counter electrode, and silver wire pseudoreference electrode were used. Potentials are referenced to an internal standard of ferrocene. For complexes **1**–**5**, no clearly defined oxidation waves were observed within the solvent window, and only the cathodic (reduction) sweep is shown. For **6**–**8**, separate anodic (black) and cathodic (red) traces were recorded, and both are plotted on the same scale. (For interpretation of the references to colour in this figure legend, the reader is referred to the web version of this article.)

of switching to NHC-based C^C: ligands is clear when looking at the CVs of complexes **6**–**8**, which all feature an irreversible but clearly observed oxidation wave. In complex **8**, which pairs the unfluorinated pmi C^C: ligand with $CNAr^{dmp}$, the anodic peak potential occurs at 1.25 V, which anodically shifts by > 300 mV to 1.66 V in complex **7** and 1.58 V in complex **8**, where the C^C: cyclometalating ligand is trifluoromethylated. The similar Ir^{IV}/Ir^{III} potentials in complexes **7** and **8** indicate that the peripheral substitution of the isocyanide has a measurable, but not large effect on the HOMO energy. We have previously noted in a larger subset of complexes with electronically modified isocyanide ligands that electron-withdrawing groups on the isocyanide can have small but measureable effects on Ir^{IV}/Ir^{III} potentials [34], which falls in line with previous work on homoleptic group 6 hexakis(aryl isocyanide) complexes [44]. That said, the effects are modest, and Figueroa et al. have shown that substitution of aryl isocyanides with electron-withdrawing groups has very small impacts on the electronic nature of the isocyanide [45].

The complexes all contain one or more irreversible reduction waves in their CVs, occurring at negative potentials beyond −1.6 V. These potentials do seem to be responsive to the number of electron-withdrawing groups on the cyclometalating ligand, suggesting that the LUMO is a π^* orbital on the cyclometalating ligand, as is typically the case for cyclometalated iridium complexes [1]. The responsiveness of the peak cathodic potential to the electron-deficiency of the cyclometalating ligand is best observed by comparing the pairs **4**/**5** and **7**/**8**. In complex **4**, the cyclometalating ligand is CF_3ptz, with a single electron-withdrawing CF_3 group, and the first reduction occurs with a peak potential of −2.33 V, shifting to a much more positive potential of −1.68 V in complex **5**, where each C^N ligand includes an additional CF_3 group. Similarly, although not as pronounced, pmi complex **8** has a reduction potential of −2.71 V, the most negative value in the series, which shifts positively to −2.64 V in complex **7**, where a CF_3 group has been added to each pmi ligand but the isocyanide is the same. In complex **6**, where the CF_3pmi C^C: ligand is paired with $CNAr^{4\text{-}CF3}$, the reduction potential shifts substantially to −2.28 V, suggesting that in this compound the LUMO could be localized on the isocyanide and not on the C^C: ligand. Taken together, the redox potentials of these compounds indicate large HOMO–LUMO gaps of at least 3.3 eV in each case, a requisite feature for designing deep-blue phosphorescent compounds.

3.4. Photophysics

The UV–vis absorption spectra and photoluminescence properties of all eight compounds were measured and are discussed herein. Overlaid UV–vis absorption spectra and photoluminescence spectra are shown in Fig. 3, and the data are summarized

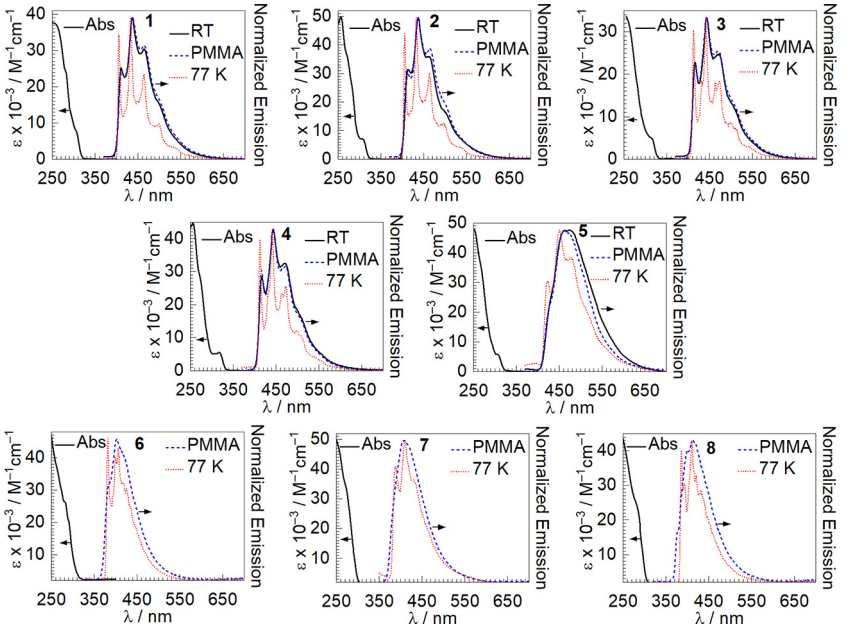

Fig. 3. Overlaid UV–vis absorption and photoluminescence spectra of complexes **1**–**8**. UV–vis absorption spectra (black solid line) were recorded in CH_2Cl_2 at room temperature, and photoluminescence spectra are shown in CH_2Cl_2 at room temperature (black solid line), 2 wt% PMMA thin film at room temperature (blue dashed line), and in CH_2Cl_2/toluene glass at 77 K (red dotted line). Excitation wavelengths for photoluminescence are 280 nm for **6**–**8** and 300–320 nm for **1**–**5**. (For interpretation of the references to colour in this figure legend, the reader is referred to the web version of this article.)

Table 1
Summary of photophysical data for complexes **1**–**8**.

	UV–vis Absorption	Photoluminescence						
	λ/nm (ε × 10^{-3}/$M^{-1}cm^{-1}$)	CH_2Cl_2, RT			77 K	PMMA, RT		
		λ/nm	Φ_{PL}	τ/μs	λ/nm	λ/nm	Φ_{PL}	(CIEx, CIEy)
1	257 (37), 282 (24), 307 (8.8)	411, 436, 464, 499(sh)	0.056	17	405, 432, 464, 498, 539(sh)	411, 437, 465, 502(sh)	0.26	(0.16, 0.14)
2	257 (50), 272 (35), 282 (26), 309 (7.3)	410, 436, 465, 502(sh)	0.031	21	405, 432, 463, 496, 540(sh)	413, 436, 464, 502(sh)	0.30	(0.16, 0.13)
3	259 (33), 282 (18), 316 (6.9)	416, 443, 472, 509(sh)	0.049	9.8	412, 441, 463, 473, 499, 513(sh), 540(sh)	416, 444, 468, 510(sh)	0.22	(0.16, 0.15)
4	256 (45), 273 (28), 319 (5.3)	415, 444, 472, 512(sh)	0.13	22	412, 441, 463, 473, 498, 510(sh), 539(sh)	416, 443, 471, 507(sh)	0.49	(0.16, 0.15)
5	251 (49), 293 (9.7), 308 (5.8)	470(br)	0.066	49	423, 450, 477, 519(sh), 563(sh)	465(br)	0.50	(0.17, 0.22)
6	281 (26), 291 (20)	a	a	a	381, 399, 406, 417, 426, 447(sh)	382(sh), 403, 420(sh)	0.13	(0.16, 0.07)
7	256 (47), 273 (33), 292 (10)	a	a	a	388, 410, 430(sh)	410	0.14	(0.16, 0.09)
8	283 (24)	a	a	a	386, 393, 410, 420, 431	376(sh), 399(sh), 414	0.14	(0.17, 0.09)

[a]These compounds are not luminescent at room temperature in solution.

in Table 1. All compounds reported here are colorless and only exhibit absorption in the UV region, in each case tailing off completely before 350 nm. All compounds have intense deep UV absorption attributed to intraligand π → π* transitions, and in the triazole complexes (**1**–**5**) a weaker near-UV maximum or shoulder is apparent, occurring between 307 and 319 nm, while in the NHC complexes the absorption monotonically decreases towards longer wavelengths and no clear low-energy band is located. These latter bands are attributed to an Ir(dπ) → C^N(π*) metal-to-ligand charge transfer (MLCT) transitions. On account of the strong-field isocyanide ligands which stabilize the Ir dπ orbitals and the high energy of the C^N LUMOs, these compounds have large HOMO–LUMO gaps (see discussion of cyclic voltammetry above), and the corresponding MLCT bands occur at high energy.

Triazole-derived complexes **1**–**5** are all moderately luminescent in CH_2Cl_2 solution at room temperature. In addition, all eight complexes luminesce at room temperature when immobilized at 2 wt% in a transparent poly(methyl methacrylate) film, allowing the photoluminescence features of all compounds to be evaluated and compared. The solution spectra are shown in Fig. 3 as black solid lines, and the spectra in polymer film are shown as blue dashed lines. For those compounds that emit in both solution and polymer film (**1**–**5**), the spectra in both media are nearly identical. The spectra for complexes **1**–**4** are all quite similar to one another, with three clearly resolved vibronic maxima at room temperature and a fourth that is evident as a shoulder at lower energy. In all cases the second maximum, the "0–1" transition, is the most intense, and in PMMA film it occurs at 437 nm (**1**) and 436 nm (**2**) for the F_2ptz complexes, and is slightly red-shifted to 444 nm (**3**) and 443 nm (**4**) for the CF_3ptz complexes. The spacing between the vibronic maxima, which averages ~1370 cm^{-1} for these four compounds, is consistent with aromatic C—C and C—N stretching vibrations coupled to the electronic excitation. The one complex we prepared with the $(CF_3)_2$ptz C^N ligand (**5**), which has an additional CF_3 group *ortho* to the site of cyclometalation, has a photoluminescence spectrum that is quite distinct from the rest of the triazole-based compounds. In both solution and polymer film, this compound displays a broad, featureless photoluminescence spectrum that is not as deep in the blue range, with a maximum at 470 nm (CH_2Cl_2 solution) and 465 nm (PMMA film). Although

the origin of this difference in spectral properties is not entirely clear from the available data, we do note that complex **5** is the easiest to reduce in the series and thus has the highest electron affinity (see Fig. 2). Thus, we presume that the red-shifted luminescence in **5** is a result of the shift in frontier orbital energies in this compound, and the broad, featureless appearance suggests there is more charge-transfer character in its excited state.

Compared to the triazole-based complexes, the NHC-based complexes **6**–**8** all have much deeper blue photoluminescence. In these compounds the vibronic structure is not clearly resolved at room temperature, but they all do have a vibronic shoulder apparent below 400 nm, and their peak maxima are > 30 nm blue-shifted from those of the F_2ptz and CF_3ptz complexes. The spectral profiles of complex **8** (C^C: = pmi) and its CF_3-substituted analogues **6** and **7** are minimally different from one another, suggesting that the addition of CF_3 substituents to the cyclometalated aryl ring does not substantially perturb the energy of the emissive triplet state.

For the compounds that do emit in solution (**1**–**5**) the quantum yields are modest, spanning 0.031 (**2**) to 0.13 (**4**). We recorded excitation spectra for these five compounds as well, which overlay perfectly with their UV–vis absorption spectra, ruling out luminescence from an impurity (see Figs. S1–S5 in the Supplementary Information). Photoluminescence lifetimes were also measured for the compounds that luminesce in solution, and they are in the usual range for cationic bis-isocyanide cyclometalated iridium complexes [33,34]. For complexes **1**–**4** the lifetimes span 9.8 and 22 μs, with a value for complex **5** (49 μs) that is longer than we typically observe for complexes in this class. When immobilized in PMMA film the quantum yields are augmented by a factor of 4 or more, a phenomenon we have observed in many other cyclometalated iridium complexes [46]. Quantum yields approaching 0.5 were observed for triazole-based compounds **4** and **5**, and in the deeper-blue phosphorescent NHC compounds more modest quantum yields are noted, 0.13 (**6**) and 0.14 (**7** and **8**). Also shown in Fig. 3 (red dotted lines) are spectra recorded at 77 K in rigid, transparent solvent glass. All compounds have very well-resolved vibronic structure at 77 K, and the complex pattern in some of the compounds, in particular **3**, **4**, **6**, and **8**, suggests that there may be two or more superimposed vibronic progressions resolved at the lower temperature. In complexes **1**–**5**, which luminesce at room temperature in fluid solution and in rigid solvent glass at 77 K, the peak maxima are generally quite similar in both media, with rigidochromic blue shifts of ~5 nm or less in each case. These small shifts indicate that the emissive triplet state in these compounds is primarily a C^N-centered intraligand, $^3(\pi \rightarrow \pi^*)$ state, with minimal charge-transfer character, falling in line with other cationic bis-isocyanide cyclometalated iridium complexes we have prepared [33,34]. The one exception to this trend is $(CF_3)_2$ptz complex **5**, which in addition to broad and featureless luminescence at room temperature experiences a substantial blue-shift in the spectral profile in rigid medium at 77 K, further suggesting enhanced charge-transfer character in this compound.

Our primary goal in this work was to design blue-phosphorescent compounds, and to examine the ability of isocyanide ligands to support robust phosphorescence in the blue region. To better contextualize the color profiles of these compounds, CIE 1931 coordinates [47], determined from the thin film photoluminescence data, are summarized in Table 1 and in Fig. 4 below. In general, the color profile is determined by the choice of the cyclometalating ligand, with very little influence of the isocyanide. The small effect of the isocyanide is unsurprising; even though the HOMO energy (and hence the HOMO–LUMO gap) can be slightly modulated by the electronic nature of the isocyanide, the emissive triplet state in these compounds is primarily ^{3}LC ($^3(\pi \rightarrow \pi^*)$) in nature with minimal participation of the HOMO, so subtle modulation of the HOMO energy does not perturb the triplet-state energy. We

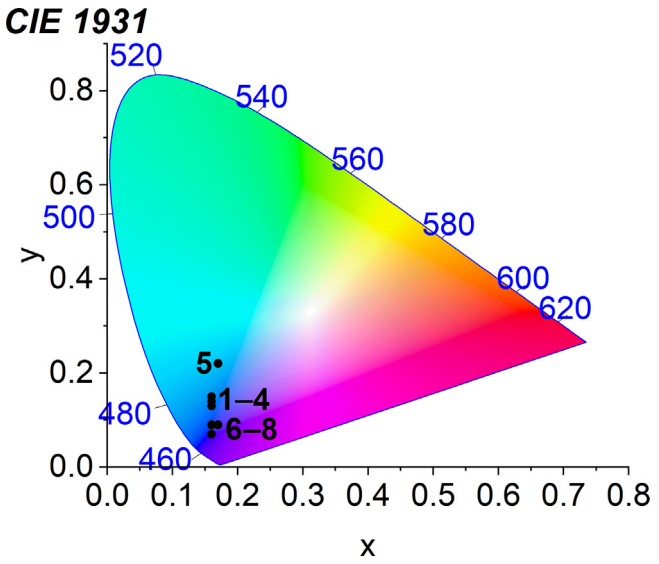

Fig. 4. Chromaticity diagram showing the (CIEx, CIEy) coordinates of **1**–**8**.

established this principle previously on a much larger set of bis(aryl isocyanide) compounds, along with the empirical observation that the nature of the isocyanide has negligible effects on the photoluminescence color [33,34]. Complex **5**, where the cyclometalating ligand is $(CF_3)_2$ptz, exhibits sky blue luminescence with (CIEx, CIEy) = (0.17, 0.22). All the rest of the triazole compounds have CIEy < 0.2 and can be classified as pure blue emitters, with (CIEx, CIEy) = (0.16, 0.13–0.15) for complexes **1**–**4**. NHC-based compounds **6**–**8** all have CIEy values of less than 0.1, and thus can be classified as deep-blue emitters. We have previously prepared complexes supported by the C^N cyclometalating ligand 2-(2,4-difluorophenyl)pyridine (F_2ppy), identical to F_2ptz but with a pyridine L donor instead of a triazole. The photoluminescence spectra of $[Ir(F_2ptz)_2(CNAr)_2]^+$ compounds **1** and **2** are slightly blue-shifted relative to analogous $[Ir(F_2ppy)_2(CNAr)_2]^+$ complexes [33], indicating that the 1,2,4-triazolyl moiety is moderately effective at blue-shifting the photoluminescence. The compounds with C^N = CF_3ptz, **3** and **4**, have almost identical photoluminescence spectra as their F_2ppy analogues, though they offer one potential advantage in electroluminescent devices, in that they lack sp^2 C–F bonds, previously shown to be prone to degradation under device operating conditions [48]. The biggest effect on the color profile was replacing the triazole-based C^N cyclometalating ligands with the NHC-based C^C: cyclometalating ligands, which shifts the photoluminescence deep into the blue range, as we [29] and many others [20,21,39] have noted in related compounds with the same cyclometalating ligands.

4. Conclusions

In this work we described eight blue-phosphorescent bis-cyclometalated iridium complexes of the general formula $[Ir(C^Y)_2(CNAr)_2]^+$, where C^Y is a triazolyl or NHC-based cyclometalating ligand, and CNAr is an aryl isocyanide. These compounds represent rare examples of heteroleptic bis-cyclometalated structures using these cyclometalating ligands, and offer a new and promising class of blue emitters. The combination of ligands in these compounds engenders them with large HOMO–LUMO gaps; the π-acidic isocyanides stabilize the Ir dπ HOMOs, and the triazole or NHC moieties present comparatively high-energy π* LUMOs. The compounds all phosphoresce in the blue region of the spectrum when excited in the UV, and in polymer films all have

moderate to good quantum yields. The photoluminescence spectral profile is principally determined by the identity of the cyclometalating ligand, with very little dependence on the isocyanide. In this way, we can span a range of blue emission hues, from sky blue to deep blue. Even though the isocyanide plays a minimal role in determining the photoluminescence of these compounds, the analogues where CNAr is the electron-accepting 4-trifluoromethylphenyl isocyanide ($CNAr^{4\text{-}CF3}$) should be amenable to nucleophilic addition reactivity to generate acyclic carbenes [27–29], and we are currently exploring the reactivity of these compounds to access a more diverse range of carbene-containing structures.

CRediT authorship contribution statement

Louise M. Cañada: Conceptualization, Methodology, Investigation, Writing - original draft, Writing - review & editing, Visualization. **Johanna Kölling:** Methodology, Investigation, Writing - original draft, Writing - review & editing, Visualization. **Thomas S. Teets:** Conceptualization, Writing - original draft, Writing - review & editing, Visualization, Supervision, Project administration, Funding acquisition.

Declaration of Competing Interest

The authors declare that they have no known competing financial interests or personal relationships that could have appeared to influence the work reported in this paper.

Acknowledgements

The authors thank the National Science Foundation (grant number CHE-1846831) and the Welch Foundation (grant number E-1887) for funding this research.

Appendix A. Supplementary data

Supplementary data to this article can be found online at https://doi.org/10.1016/j.poly.2019.114332.

References

[1] E. Zysman-Colman (Ed.), Iridium(III) in Optoelectronic and Photonics Applications, John Wiley & Sons Inc, Chichester, West Sussex, 2017.
[2] H. Yersin (Ed.), Highly Efficient OLEDs with Phosphorescent Materials, WILEY-VCH, Weinheim, 2008.
[3] S. Sprouse, K.A. King, P.J. Spellane, R.J. Watts, Photophysical effects of metal-carbon σ bonds in ortho-metalated complexes of iridium(III) and rhodium(III), J. Am. Chem. Soc. 106 (1984) 6647–6653, https://doi.org/10.1021/ja00334a031.
[4] K.A. King, R.J. Watts, Dual emission from an ortho-metalated iridium(III) complex, J. Am. Chem. Soc. 109 (1987) 1589–1590, https://doi.org/10.1021/ja00239a060.
[5] K. Dedeian, P.I. Djurovich, F.O. Garces, G. Carlson, R.J. Watts, A new synthetic route to the preparation of a series of strong photoreducing agents: *fac*-tris-ortho-metalated complexes of iridium(III) with substituted 2-phenylpyridines, Inorg. Chem. 30 (1991) 1685–1687, https://doi.org/10.1021/ic00008a003.
[6] M.A. Baldo, S. Lamansky, P.E. Burrows, M.E. Thompson, S.R. Forrest, Very high-efficiency green organic light-emitting devices based on electrophosphorescence, Appl. Phys. Lett. 75 (1999) 4–6, https://doi.org/10.1063/1.124258.
[7] A. Tsuboyama, H. Iwawaki, M. Furugori, T. Mukaide, J. Kamatani, S. Igawa, T. Moriyama, S. Miura, T. Takiguchi, S. Okada, M. Hoshino, K. Ueno, Homoleptic cyclometalated iridium complexes with highly efficient red phosphorescence and application to organic light-emitting diode, J. Am. Chem. Soc. 125 (2003) 12971–12979, https://doi.org/10.1021/ja034732d.
[8] S. Lamansky, P. Djurovich, D. Murphy, F. Abdel-Razzaq, H.-E. Lee, C. Adachi, P.E. Burrows, S.R. Forrest, M.E. Thompson, Highly phosphorescent bis-cyclometalated iridium complexes: synthesis, photophysical characterization, and use in organic light emitting diodes, J. Am. Chem. Soc. 123 (2001) 4304–4312, https://doi.org/10.1021/ja003693s.
[9] Y. You, S.Y. Park, Inter-ligand energy transfer and related emission change in the cyclometalated heteroleptic iridium complex: facile and efficient color tuning over the whole visible range by the ancillary ligand structure, J. Am. Chem. Soc. 127 (2005) 12438–12439, https://doi.org/10.1021/ja052880t.
[10] Y.-J. Su, H.-L. Huang, C.-L. Li, C.-H. Chien, Y.-T. Tao, P.-T. Chou, S. Datta, R.-S. Liu, Highly efficient red electrophosphorescent devices based on iridium isoquinoline complexes: remarkable external quantum efficiency over a wide range of current, Adv. Mater. 15 (2003) 884–888, https://doi.org/10.1002/adma.200304630.
[11] C.-H. Fan, P. Sun, T.-H. Su, C.-H. Cheng, Host and dopant materials for idealized deep-red organic electrophosphorescence devices, Adv. Mater. 23 (2011) 2981–2985, https://doi.org/10.1002/adma.201100610.
[12] Y.K. Radwan, A. Maity, T.S. Teets, Manipulating the excited states of cyclometalated iridium complexes with β-ketoiminate and β-diketiminate ligands, Inorg. Chem. 54 (2015) 7122–7131, https://doi.org/10.1021/acs.inorgchem.5b01401.
[13] P.-N. Lai, C.H. Brysacz, M.K. Alam, N.A. Ayoub, T.G. Gray, J. Bao, T.S. Teets, Highly efficient red-emitting bis-cyclometalated iridium complexes, J. Am. Chem. Soc. 140 (2018) 10198–10207, https://doi.org/10.1021/jacs.8b04841.
[14] P. Lai, T.S. Teets, Ancillary ligand effects on red-emitting cyclometalated iridium complexes, Chem. Eur. J. 25 (2019) 6026–6037, https://doi.org/10.1002/chem.201900829.
[15] R.M. Maya, A. Maity, T.S. Teets, Fluorination of cyclometalated iridium β-ketoiminate and β-diketiminate complexes: extreme redox tuning and ligand-centered excited states, Organometallics 35 (2016) 2890–2899, https://doi.org/10.1021/acs.organomet.6b00453.
[16] J. Li, P.I. Djurovich, B.D. Alleyne, M. Yousufuddin, N.N. Ho, J.C. Thomas, J.C. Peters, R. Bau, M.E. Thompson, Synthetic control of excited-state properties in cyclometalated Ir(III) complexes using ancillary ligands, Inorg. Chem. 44 (2005) 1713–1727, https://doi.org/10.1021/ic048599h.
[17] M.S. Lowry, S. Bernhard, Synthetically tailored excited states: phosphorescent, cyclometalated iridium(III) complexes and their applications, Chem. Eur. J. 12 (2006) 7970–7977, https://doi.org/10.1002/chem.200600618.
[18] R.J. Holmes, S.R. Forrest, T. Sajoto, A. Tamayo, P.I. Djurovich, M.E. Thompson, J. Brooks, Y.-J. Tung, B.W. D'Andrade, M.S. Weaver, R.C. Kwong, J.J. Brown, Saturated deep blue organic electrophosphorescence using a fluorine-free emitter, Appl. Phys. Lett. 87 (2005), https://doi.org/10.1063/1.2143128 243507.
[19] T. Sajoto, P.I. Djurovich, A. Tamayo, M. Yousufuddin, R. Bau, M.E. Thompson, R. J. Holmes, S.R. Forrest, Blue and near-UV phosphorescence from iridium complexes with cyclometalated pyrazolyl or *N*-heterocyclic carbene ligands, Inorg. Chem. 44 (2005) 7992–8003, https://doi.org/10.1021/ic051296i.
[20] J. Lee, H.-F. Chen, T. Batagoda, C. Coburn, P.I. Djurovich, M.E. Thompson, S.R. Forrest, Deep blue phosphorescent organic light-emitting diodes with very high brightness and efficiency, Nat. Mater. 15 (2015) 92–98, https://doi.org/10.1038/nmat4446.
[21] A.K. Pal, S. Krotkus, M. Fontani, C.F.R. Mackenzie, D.B. Cordes, A.M.Z. Slawin, I. D.W. Samuel, E. Zysman-Colman, High-efficiency deep-blue-emitting organic light-emitting diodes based on iridium(III) carbene complexes, Adv. Mater. 30 (2018) 1804231, https://doi.org/10.1002/adma.201804231.
[22] Z. Chen, L. Wang, S. Su, X. Zheng, N. Zhu, C.-L. Ho, S. Chen, W.-Y. Wong, Cyclometalated iridium(III) carbene phosphors for highly efficient blue organic light-emitting diodes, ACS Appl. Mater. Interfaces 9 (2017) 40497–40502, https://doi.org/10.1021/acsami.7b09172.
[23] H. Sasabe, J. Takamatsu, T. Motoyama, S. Watanabe, G. Wagenblast, N. Langer, O. Molt, E. Fuchs, C. Lennartz, J. Kido, High-efficiency blue and white organic light-emitting devices incorporating a blue iridium carbene complex, Adv. Mater. 22 (2010) 5003–5007, https://doi.org/10.1002/adma.201002254.
[24] K.-Y. Lu, H.-H. Chou, C.-H. Hsieh, Y.-H.O. Yang, H.-R. Tsai, H.-Y. Tsai, L.-C. Hsu, C.-Y. Chen, I.-C. Chen, C.-H. Cheng, Wide-range color tuning of iridium biscarbene complexes from blue to red by different N_iN ligands: an alternative route for adjusting the emission colors, Adv. Mater. 23 (2011) 4933–4937, https://doi.org/10.1002/adma.201102886.
[25] C.-H. Hsieh, F.-I. Wu, C.-H. Fan, M.-J. Huang, K.-Y. Lu, P.-Y. Chou, Y.-H.O. Yang, S.-H. Wu, I.-C. Chen, S.-H. Chou, K.-T. Wong, C.-H. Cheng, Design and synthesis of iridium bis(carbene) complexes for efficient blue electrophosphorescence, Chem. Eur. J. 17 (2011) 9180–9187, https://doi.org/10.1002/chem.201100317.
[26] C.-F. Chang, Y.-M. Cheng, Y. Chi, Y.-C. Chiu, C.-C. Lin, G.-H. Lee, P.-T. Chou, C.-C. Chen, C.-H. Chang, C.-C. Wu, Highly efficient blue-emitting iridium(III) carbene complexes and phosphorescent OLEDs, Angew. Chem. Int. Ed. 47 (2008) 4542–4545, https://doi.org/10.1002/anie.200800748.
[27] H. Na, T.S. Teets, Highly luminescent cyclometalated iridium complexes generated by nucleophilic addition to coordinated isocyanides, J. Am. Chem. Soc. 140 (2018) 6353–6360, https://doi.org/10.1021/jacs.8b02416.
[28] H. Na, A. Maity, R. Morshed, T.S. Teets, Bis-cyclometalated iridium complexes with chelating dicarbene ancillary ligands, Organometallics 36 (2017) 2965–2972, https://doi.org/10.1021/acs.organomet.7b00428.
[29] H. Na, L.M. Cañada, Z. Wen, J. I-Chia Wu, T.S. Teets, Mixed-carbene cyclometalated iridium complexes with saturated blue luminescence, Chem. Sci. 10 (2019) 6254–6260. doi: 10.1039/C9SC01386E.
[30] S.-C. Lo, C.P. Shipley, R.N. Bera, R.E. Harding, A.R. Cowley, P.L. Burn, I.D.W. Samuel, Blue phosphorescence from iridium(III) complexes at room temperature, Chem. Mater. 18 (2006) 5119–5129, https://doi.org/10.1021/cm061173b.
[31] S.-C. Lo, R.E. Harding, C.P. Shipley, S.G. Stevenson, P.L. Burn, I.D.W. Samuel, High-triplet-energy dendrons: enhancing the luminescence of deep blue

phosphorescent iridium(III) complexes, J. Am. Chem. Soc. 131 (2009) 16681–16688, https://doi.org/10.1021/ja903157e.
[32] S.-C. Lo, R.N. Bera, R.E. Harding, P.L. Burn, I.D.W. Samuel, Solution-processible phosphorescent blue dendrimers based on biphenyl-dendrons and *Fac*-tris (phenyltriazolyl)iridium(III) cores, Adv. Funct. Mater. 18 (2008) 3080–3090, https://doi.org/10.1002/adfm.200800658.
[33] A. Maity, L.Q. Le, Z. Zhu, J. Bao, T.S. Teets, Steric and electronic influence of aryl isocyanides on the properties of iridium(III) cyclometalates, Inorg. Chem. 55 (2016) 2299–2308, https://doi.org/10.1021/acs.inorgchem.5b02691.
[34] H. Na, A. Maity, T.S. Teets, Bis-cyclometalated iridium complexes with electronically modified aryl isocyanide ancillary ligands, Dalton Trans. 46 (2017) 5008–5016, https://doi.org/10.1039/C7DT00694B.
[35] K. Dedeian, J. Shi, E. Forsythe, D.C. Morton, P.Y. Zavalij, Blue phosphorescence from mixed cyano-isocyanide cyclometalated iridium(III) complexes, Inorg. Chem. 46 (2007) 1603–1611, https://doi.org/10.1021/ic061513v.
[36] N.M. Shavaleev, F. Monti, R.D. Costa, R. Scopelliti, H.J. Bolink, E. Ortí, G. Accorsi, N. Armaroli, E. Baranoff, M. Grätzel, M.K. Nazeeruddin, Bright blue phosphorescence from cationic bis-cyclometalated iridium(III) isocyanide complexes, Inorg. Chem. 51 (2012) 2263–2271, https://doi.org/10.1021/ic202297h.
[37] N.M. Shavaleev, F. Monti, R. Scopelliti, N. Armaroli, M. Grätzel, M.K. Nazeeruddin, Blue phosphorescence of trifluoromethyl- and trifluoromethoxy-substituted cationic iridium(III) isocyanide complexes, Organometallics 31 (2012) 6288–6296, https://doi.org/10.1021/om300557d.
[38] N.M. Shavaleev, F. Monti, R. Scopelliti, A. Baschieri, L. Sambri, N. Armaroli, M. Grätzel, M.K. Nazeeruddin, Extreme tuning of redox and optical properties of cationic cyclometalated iridium(III) isocyanide complexes, Organometallics 32 (2013) 460–467, https://doi.org/10.1021/om300894m.
[39] T. Sajoto, P.I. Djurovich, A. Tamayo, M. Yousufuddin, R. Bau, M.E. Thompson, R. J. Holmes, S.R. Forrest, Blue and near-UV phosphorescence from iridium complexes with cyclometalated pyrazolyl or N-heterocyclic carbene ligands, Inorg. Chem. 44 (2005) 7992–8003, https://doi.org/10.1021/ic051296i.
[40] W.P. Weber, G.W. Gokel, An improved procedure for the Hofmann carbylamine synthesis of isonitriles, Tetrahedron Lett. 13 (1972) 1637–1640, https://doi.org/10.1016/S0040-4039(01)84707-9.
[41] K. Suzuki, A. Kobayashi, S. Kaneko, K. Takehira, T. Yoshihara, H. Ishida, Y. Shiina, S. Oishi, S. Tobita, Reevaluation of absolute luminescence quantum yields of standard solutions using a spectrometer with an integrating sphere and a back-thinned CCD detector, Phys. Chem. Chem. Phys. 11 (2009) 9850–9860, https://doi.org/10.1039/B912178A.
[42] G.M. Sheldrick, A short history of *SHELX*, Acta Crystallogr. A. 64 (2008) 112–122, https://doi.org/10.1107/S0108767307043930.
[43] A.L. Spek, Structure validation in chemical crystallography, Acta Crystallogr. D Biol. Crystallogr. 65 (2009) 148–155, https://doi.org/10.1107/S090744490804362X.
[44] G.J. Essenmacher, P.M. Treichel, Electrochemistry of a series of hexakis(aryl isocyanide)chromium(0) complexes, Inorg. Chem. 16 (1977) 800–806, https://doi.org/10.1021/ic50170a015.
[45] A.E. Carpenter, C.C. Mokhtarzadeh, D.S. Ripatti, I. Havrylyuk, R. Kamezawa, C.E. Moore, Arnold L. Rheingold, J.S. Figueroa, Comparative measure of the electronic influence of highly substituted aryl isocyanides, Inorg. Chem. 54 (2015) 2936–2944, https://doi.org/10.1021/ic5030845.
[46] H. Na, P. Lai, L.M. Cañada, T.S. Teets, Photoluminescence of cyclometalated iridium complexes in poly(methyl methacrylate) films, Organometallics 37 (2018) 3269–3277, https://doi.org/10.1021/acs.organomet.8b00446.
[47] T. Smith, J. Guild, The C.I.E. colorimetric standards and their use, Trans. Opt. Soc. 33 (1931) 73–134, https://doi.org/10.1088/1475-4878/33/3/301.
[48] R. Seifert, I. Rabelo de Moraes, S. Scholz, M.C. Gather, B. Lüssem, K. Leo, Chemical degradation mechanisms of highly efficient blue phosphorescent emitters used for organic light emitting diodes, Org. Electron. 14 (2013) 115–123, https://doi.org/10.1016/j.orgel.2012.10.003.